

Fig. 2. Effect of drum speed on threshing efficiency

Increasing drum speed from 500 to 700rpm under constant material feed rate of 5, 10 and 15 kg/min increase the percentage of threshing efficiency by 1.67, 1.66, and 3 %, respectively using the threshing machine under the same conditions. The increase in the percentage of threshing efficiencies by increasing drum speed are attributed to the high stripping and impacting forces applied to the soybean materials, that tends to improve the threshing operation and increase threshing efficiencies.

4.1.2 Effect of material feed rate on threshing efficiencies

Concerning the effect of material feed rate on the percentage of threshing efficiency, results obtained shows that increasing feed rate increased the percentage of threshing efficiency when feeding rate increase from 5 to 10kg/min and decreased the percentage of threshing efficiency from 10 to 15kg/min under all experimental conditions. The increase in the percentage of un-threshed grains and the decrease in percentage of threshing efficiency by increasing material feed rate are attributed to the excessive materials in the threshing chamber. Consequently, soybean plants leave the device without complete threshing that tends to increase un-threshed grains and decrease damaged grains.

4.2 Cleaning Efficiency

1.1.1. Effect of threshing drum speed on cleaning efficiency

The results in Fig. 3, illustrated that the lowest values of cleaning efficiency was obtained at drum speed of 500 rpm of threshing machines, however the highest values of cleaning efficiency was obtained at drum speed of 700 rpm at different feeding rate. The high drum speed increased the velocity of cleaning air results in higher capability of air to carry the foreign material and residual of soybean heads from seeds consequently increased cleaning efficiency. On the other words, increased the drum speeds from 500 to 600 rpm increased the cleaning efficiency by 1.33% at feeding rates of 5kg/min. However by increasing drum speed from 600 to 700 rpm increased the cleaning efficiency by 0.67% at feeding rate of about 5kg/min.

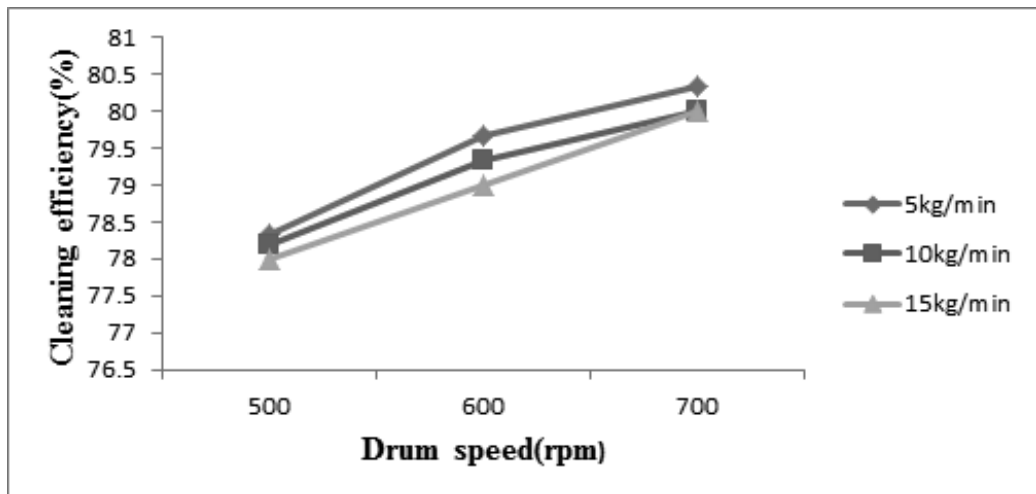


Fig. 3. Effect of drum speed on cleaning efficiency

1.1.2. Effect of feeding rate on cleaning efficiency

The results plotted in Fig. 4, indicated that the increasing feeding rate from 5 to 10 kg/min. the cleaning efficiency was decreased by 0.14, 0.33 and 0.34% at drum speed of 500 , 600 and 700rpm respectively. This is true, because the machine have oscillating sieves which greatly increase cleaning efficiency. The maximum cleaning efficiency of 80.34% was obtained when using the machine at feeding rate of 5 kg/min and 700rpm drum speed under 9% of moisture content.

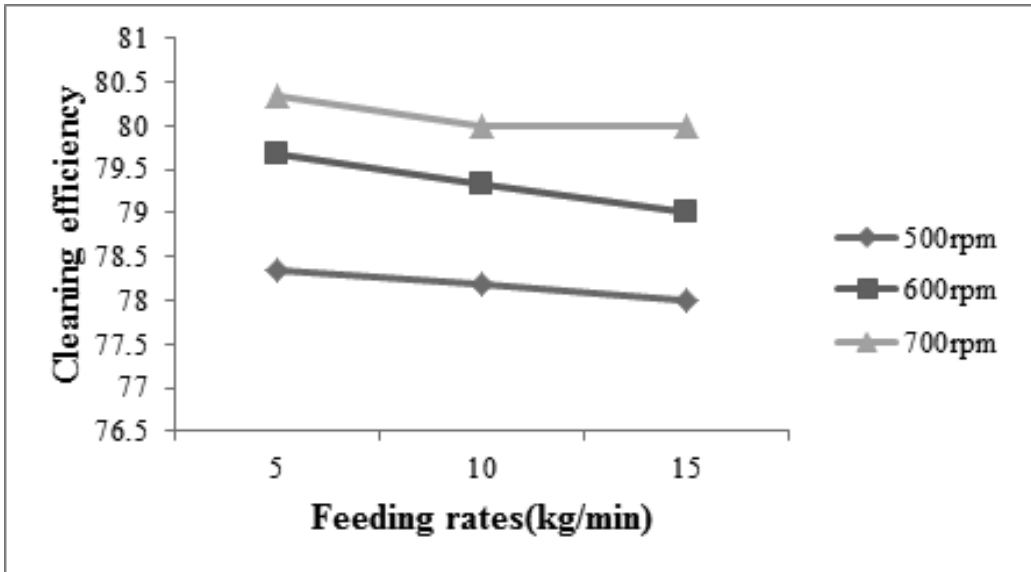


Fig. 4. Effect of feeding rates on cleaning efficiency

4.3 Threshing capacity

Figure 5 shows that, the effect of drum speed on capacity at different feed rates. The results indicated that the capacity increased with an increased in drum speed for all feed rates. And also the capacity increase with an increase of feed rates. The maximum capacity was obtained at the feed rates of 15 kg/min and at drum speed of 700 rpm.

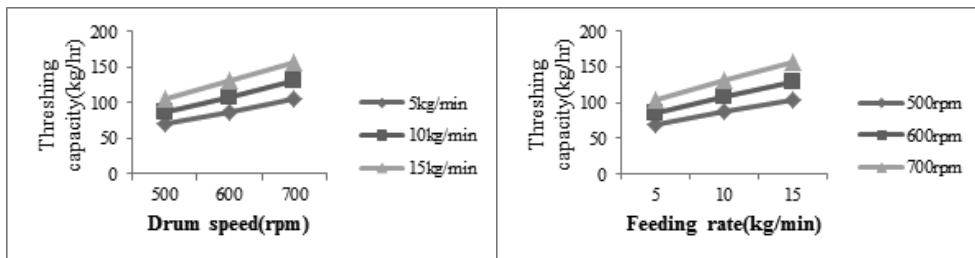


Fig. 5. Effect of drum speed and material feed rate on threshing capacity (kg/hr)

1.4 Total Seed Loss

4.4.1 Effect of drum speed

The total grain losses are the sum of un-threshed grains, damaged grains and seeds thrown out directly by oscillating sieve motion and air velocity during the threshing operation. The total losses were influenced significantly by the cylinder speed. The results

in Fig.6, illustrated that the total seed increased with increasing drum speed at different feeding rates. Also, it could be noticed that the lowest values of the total seed losses was obtained at 500 rpm drum speed of threshing machines. However, the highest values of the total seed losses were obtained at 700 rpm drum speed of threshing machines at different feeding rates. The results also cleared that at feeding rate of 5 kg/min., increasing threshing drum speed from 500 to 700 rpm increased the total seed losses from 4.07 to 4.2 %.

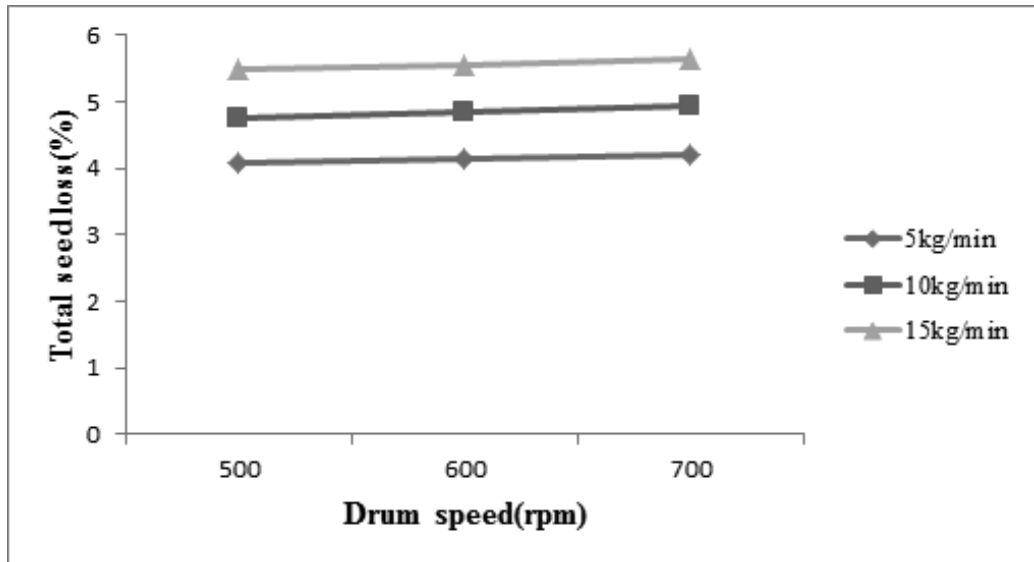


Fig.6. Effect of drum speed on total seed loss

4.4.2 Effect of feeding rate

Fig. 7, illustrated that the maximum values of total seed losses percentage of about 5.48, 5.56 and 5.63 % was obtained at feeding rate of 15 kg/min. On the other hands, increasing feeding rate from 5 to 10 kg/min at drum speed of 500rpm increased the total seed losses from 4.07 to 4.76% under 9% soybean heads moisture content.

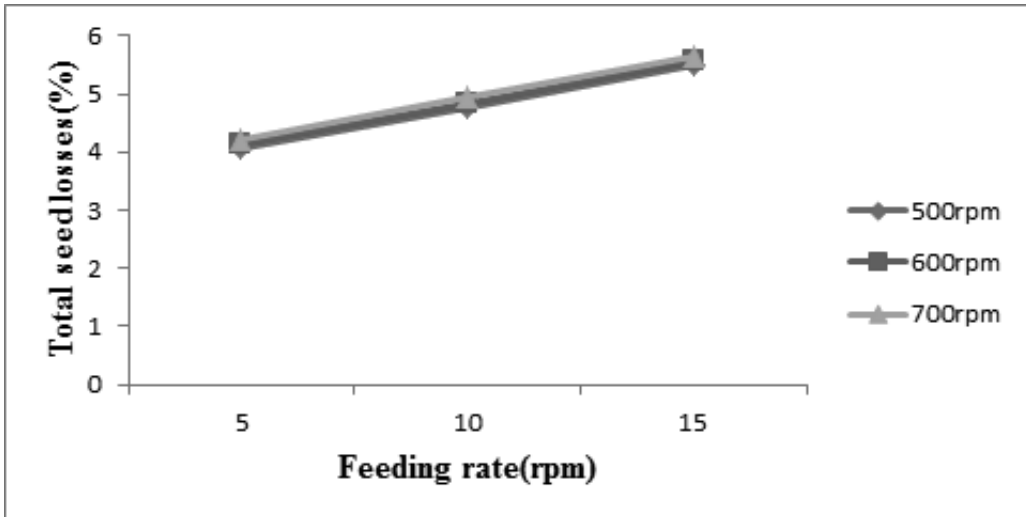


Fig.7. Effect of feeding rates on total seed loss

4.5 Seed breakage

4.5.1 Effect of threshing drum speed

The results in Fig.8. indicated that by increasing drum speed from 500 rpm to 600 rpm gave the lowest increment rate than obtained when increased the drum speed from 600 to 700 rpm. Also, it could be noticed that the lowest values of seed damage was obtained at 500rpm, however the highest values of seed damage was obtained at 700 rpm of drum speed of threshing machines at different feeding rate.

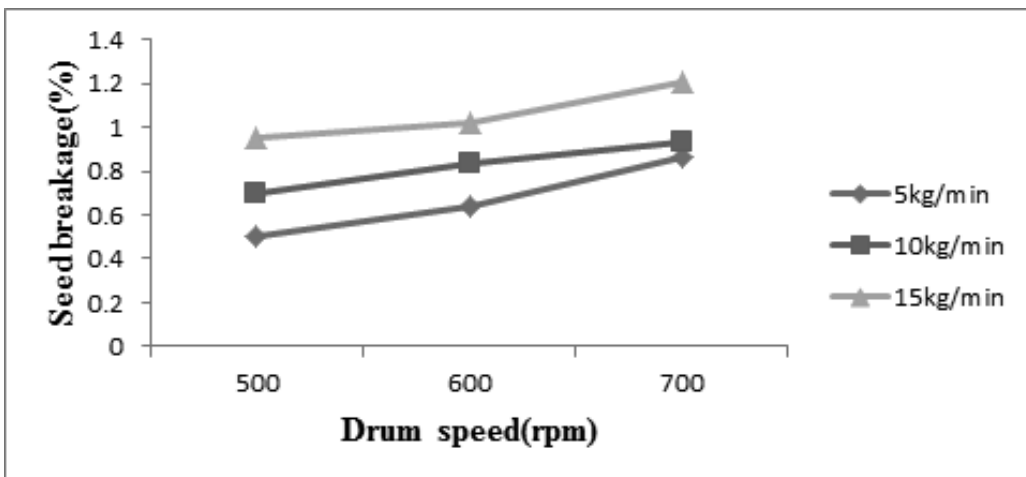


Fig.8. Effect of drum speed on seed breakage

4.5.2 Effect of feeding rate

Results in Fig. 9, illustrated that the higher values of seed damage resulted at 15kg/min of feeding rates of the machine. Increasing feeding rate from 5 to 10 kg/min. increased the seed damage by 0.2%while increasing feeding rates from 10 15kg/min increased the seed damage by 0.25 % at drum speed of 500rpm. The maximum seed damage percentage of 6.79, 5.32 and 1.56 % were occurred at feeding rate of 15 kg/min under different drum speed.

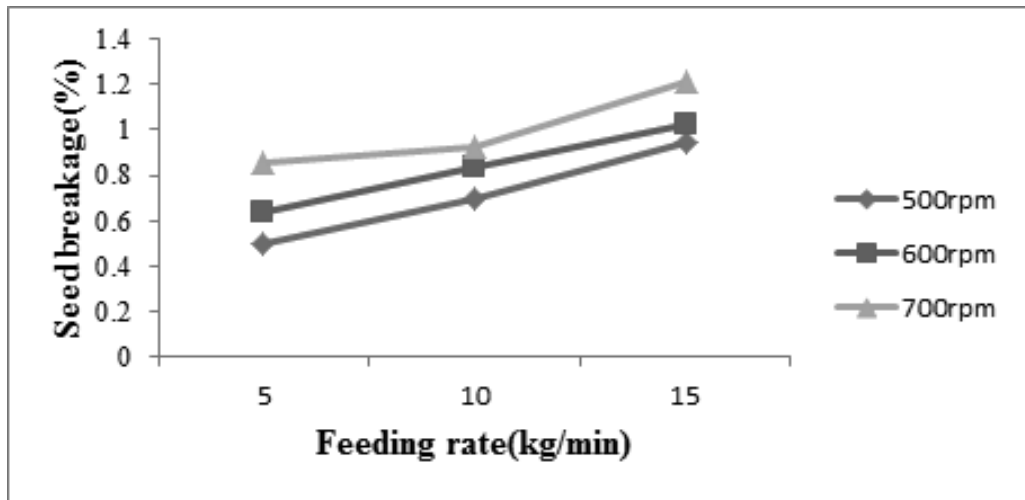


Fig.9. Effect of feeding rate on seed breakage

4.6 Summery

The following conclusions could be drawn from this study:-The performance of the modified soybean thresher was affected by the moisture content, the cylinder speed of the threshing drum as well as the feed rate. The optimum threshing efficiency of 99.87 % was obtained using the drum speed of 600 rpm, feeding rate of 5kg/min and 9 % of grain moisture content. Maximum threshing capacity of 156.84 kg/hr was obtained at drum speed of 700 rpm, 15kg/min feeding rate and 9 % of grain moisture content. Maximum Grain loss was 5.63% at drum speed of 700 rpm, 10/min feeding rate and 9 % of grain moisture content. Minimum grain loss 4.07 % at drum speed of 400 rpm 5 kg/min feeding rate and 9 % of grain moisture content. Maximum cleaning efficiency 81% at drum speed of 600 rpm, 10 kg/min feeding rate and 8 % of grain moisture content. Minimum cleaning

efficiency 78.34 % at drum speed of 400 rpm, 5 kg/min feeding rate and 9 % of grain moisture content.

4.7 Recommendation

In order to minimize damaged grain, it is recommended that to investigate the effects of other machine-crop parameters such as concave clearance, hopper inlet opening and crop variety on the performance of the thresher.

5. Reference

- Bernard, Richard L. "Soyabean," Microsoft® Encarta® Encyclopedia 2007[CD]. Redmond, WA: 1 Microsoft Corporation, 2006.
- Gomez, K. A. and A. A. Gomez. 1984. Statistical Procedures for Agricultural Research. Second Edition, John Wiley & Sons, Inc., New York.
- Newberg, R. S., M. R. Pualsen and W. R. Nave. 1980. Soybean quality with rotary and conventional threshing. Transactions of the ASAE, 23(2):303-308.
- Kaul, R. N. and C. O. Egbo (1985):** Introduction to Agricultural Mechanization. First edition. Macmillan Education Ltd. London.
- Ogoke, I. J., A. O. Togun, R. J. Carsky, K. Dashiell, 2004. Effect of Phosphorus Fertilizer on Soybean Residue Turnover in the Tropical Moist Savanna Journal of Agronomy and Crop Science 190 (6), 367–373.
- Sukprakarn S., S. Juntakool and R. Huang, 2006. saving your own vegetable seeds- a guide for farmers. Published by AVRDC.
- Vejasit. A. and V. Salokhe, 2004. "Studies on Machine-Crop Parameters of an Axial Flow Thresher for Threshing Soybean". Agriculture Engineering International: the GIGR Journal of Scientific Research and Development. Manuscript PM 04 004.
- Whighan D.K., 1974. Soybean production, protection, and utilization. Proceeding of a conference for scientists of Africa, the Middle East, and South Asia, October 14-17, Addis Ababa, Ethiopia.

Adaptation and Promotion of Agro Saw Seed Cleaner

Ashebir T., Alemneh H., Gosa B., Efrem B., and Dinqa F.

Oromia Agricultural Research Institute, Asalla Agricultural Engineering Research Center

ABSTRACT

The machine has over all dimensions of length, width and height 2400 mm, 1400 mm and 2800 mm respectively. The cleaning system consists of an air blast fan and a reciprocating shaker containing replaceable sieve for different crop seeds. The cleaning operation is powered by electric motor to drive cam shaft, fane and grain elevator. The developed cleaning machine had the ability to clean the pre-mature grains, chaff and leaves, which are lighter than grains. The performance of the adapted prototype was evaluated in terms of percentage cleaning efficiency and cleaning capacity at various levels of feed rates. The test crops used was wheat. The best performance was obtained 99.07% and 19.2 quintal/h of cleaning efficiency and capacity respectively for wheat grains.

1. INTRODUCTION

Agriculture is the largest single industry in the world, and seed production is an important segment of this industry. In traditional method, about 40% of the total labor required to produce crop is extended in threshing, cleaning and transportation activities (Johnson, 1992). The average post-harvest losses of food crops such as Teff, Wheat and Maize are annually 12.9%, 13.6% and 10.9% respectively (Derege A. et al 1989). Among this cleaning by rational method has many loss of grain.

Cleaning of grain or winnowing is one of the important postharvest processes done in preparing seeds/grains as food or any industrial raw material. It involves the removal of chaff and other debris from the grain. There are quite a number of factors that affect the performance in terms of cleanliness and grain loss during the operation. Such factors include amount of wind or air velocity, feed rate, shaker frequency, dimension of sieve opening, sieve tilt angle, crop variety and moisture content (Sharma, 1976).

In Ethiopia, grain cleaning i.e. removal of undesirable materials, is accomplished manually by tossing the grain into air and letting the wind do the separation and cleaning, removal of lightest impurities, leaves and large amount of debris with certain amount of grains. In certain circumstances, the velocity of the wind may be too low so that heavier impurities (gravel, ear, chaff, etc.) remain mixed with the grains. These contaminants must be removed, and the clean seed properly

handled and stored to provide a high quality planting seed that will increase farm production and supply uniform raw material for industry.

In Ethiopia, seed/grain cleaning is part of women's contribution in processing of grains. A circular tray made from the grass so called 'sindedo' of stalk is used. The long hours associated with the traditional method results in fatigue, loss of concentration and consequently, reduction in separation quality. So often the natural wind condition may not be favorable for the operation and the result is increased time of operation and drudgery. Especially, seed producer cooperatives, governmental seed enterprises, state farms and agricultural research centers are facing problems of seed cleaning and most of them are processing their seed manually and the others import the machine from abroad by expensive hard currency. Even the machine has been installed by the experts coming from the manufacturing company.

Seed cleaning can be accomplished by using pneumatic separators, screen cleaners, or gravity tables. Many commercial cleaners incorporate more than one of these cleaning methods (Hauhouotet *al.*, 2000). In general seed processing has four stages namely, rough cleaning, pre-cleaning, industrial cleaning and fine cleaning. Rough-cleaning, on the other hand, is a process in which material both larger and smaller than the crop seed is removed. Pre-cleaning or rough-cleaning is now regarded as a basic operation by many seeds men, because seed harvested with modern combines are often heavily contaminated with foreign material such as sticks, stems, leaves, trash and weed seeds. This material, which may be as much as 60 to 70 percent of the volume of the combine run seed lot, needs to be removed before seed can be safely stored, effectively cleaned.

This stage is, as the first entrance for further seed processing and grading, is very important and requires huge labor and consumes more time when it is operated manually. Especially, seed producer cooperatives, governmental seed enterprises, state farms and agricultural research centers are facing problems of seed cleaning and most of them are processing their seed manually and the others import the machine from abroad by expensive hard currency. Even the machine has been installed by the engineers coming from the manufacturing company.

Hence, this project was initiated to bridge the existing technology gaps in the area of seed cleaner, with prime objective of adopt and manufacture the AGROSAW (Model-PC-3) seed cleaner and conduct promotion with the following specific objectives:-

1. To adapt AGROSAW (Model-PC-3) pre-cleaner and make performance evaluation of the machine at station.
2. To promote the adopted technology for selected governmental and non-gov-

ernmental organizations

3. To create awareness among seed enterprise, research centers, etc. to raise their perception on the technology.

2. Materials and Methods

2.1 Description of the Machine

The major components of the machine are the frame, grain elevator bucket, hoppers, dust collectors, pulleys and V-belts, separating and cleaning unit, electrical motors, eccentric wheel, fan and fan housing. Figure 1 gives details of machine developed, constructed and used in the experiment. (Photograph of the cleaning machine).



Figure 1. Grain cleaning machine

2.1.1 Bucket elevator

The bucket elevator consists of buckets attached to an endless belt which runs along a vertical path. The system would be enclosed in separate housings for the lift leg and return leg. The buckets load themselves as they pass through a seed hopper or “*boot” at the bottom of the run, and, depending upon elevator type, the load is discharged by centrifugal force or gravity as the buckets round the top section of the assembly. The centrifugal-discharge elevator is commonly operated at high speeds to obtain high capacities, and the resultant discharge velocity may cause excessive damage to injury sensitive seed. Slow-speed units are better for easily damaged or slow-flowing materials. Another limitation of bucket elevators is that they are difficult to clean. Small seeds tend to lodge in hard-to-clean areas throughout the elevator and remain there to contaminate subsequent lots.

2.1.2 Power source

The following electric motors were installed in the frame of the cleaning unit.

Cam Shaft Drive: - Single face electric motor, 1.1 KW, 1.5 HP, 220 V, 1420 rpm, 50Hz, 10.4 A, Anti clockwise rotation.

Fan Shaft Drive: - Single face electric motor, 2.2 K.W, 3HP, 220 V, 1450 Rpm, 50Hz, 13 A, Anti clockwise rotation.

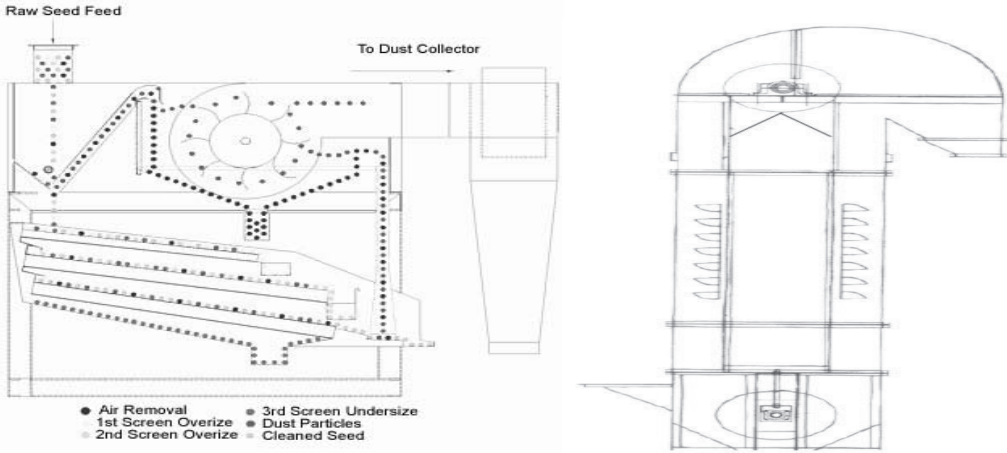
Grain Elevator Drive: - Single face electric motor, 1.1 KW, 1.5 HP, 220 V, 1420 Rpm 50Hz, 6.6 A, Anti clockwise rotation.

2.1.3 Selecting Screens

The two basic screens for cleaning round-shaped seed are a round-hole top screen and a slotted bottom screen. The round-hole top screen should be selected so as to drop the round seed through the smallest hole possible, and retain anything larger. The seed drops through the top screen onto the slotted bottom screen, which takes advantage of seed shape and retains the round, good seed while dropping broken crop seed and many weed seed. The basic screens for cleaning elongated seed are a slotted top screen and a slotted bottom screen. In special separations it may be necessary to pass such seed through round hole top screens or over some screen other than a slotted bottom screen, but generally, slotted top and bottom screens are used.

2.1.4 Operation system of the Machine

The grains seed lifted by elevator bucket from the ground vertically upward and discharge it from top to the machine hopper where they are evenly distributed by a feed roller and transferred through a controlled gate on the top sieve. In the process the grains are subjected to primary aspiration by the use of air trunk which drains off chaff, straw, dust or decreased grains. Then the material is passed through sieve layer for separation according to their width and thickness. After the separation, the graded material is subjected to air lifter and aspiration chamber where remaining light particles are sucked off by a strong upward draught of air. The graded material and the impurities are automatically discharged in separate chutes.



Cross sectional view of the machine and grain elevator

2.2 Performance Evaluation

The test involves taking randomly selected three samples which were at the grain outlet and the non-grain (unwanted material) outlet. The weights of grain and other material in each sample were recorded. The procedure was repeated for each throughput. The amount of debris in clean grain outlet samples determined the cleanliness (cleaning efficiency) while the amount of grain found in non-grain outlet samples determines the grain loss. The expressions used for calculating the percent cleaning efficiency and percent grain loss were as follows:

$$\eta = \frac{G_o}{G_o + C_{cg}} \times 100$$

Where:-

η = cleaning efficiency, %

G_o = weight of pure grain at the outlet, g.

C_{cg} = weight of contaminant in cleaned grain, g.

$$C_L = \frac{G_i}{G_w} \times 100$$

Where:-

G_i = weight of grain at the chaff outlet, g.

G_w = weight of grain at input, g.

C_L = cleaning loss,

2.2.1 Mechanical Seed Damage

Seeds can suffer mechanical injury in any handling operation that provides a chance for abrasion or impact to occur. The injury may not be evident immediately, either visually or by germination tests, but may appear later in the form of reduced storage life and poor field germination.

2.2.2 Method of promotion

To conduct the promotion of seed cleaning technology to seed producer, research centers, farmers unions' and respective organizations were purposively selected based on their seed producing potential and accessibility. From these selected organizations two respective persons were invited to attend field days organized at Asella Agricultural Mechanization research center by panel discussions for one day.

3. Result and Discussions

The machine was fabricated at AAMRC on the basis of the manufacturer specifications. The physical attributes of grain was used for selection of sieve opening sizes required to effect the cleaning of the grain. Oscillations of the sieves were made by using a four-bar linkage mechanism where the legs of the sieve holding frame were pinned and oscillated about a vertical plane.

3.1 Capacity of the machine

Capacity of the cleaner varies depending upon the crop, contaminants and grade desired, Best results with the samples tested were obtained with incoming feed rates of 19.2 quintals / hour and 99.07 % cleaning efficiency in Wheat crop whereas the cleaning capacity of imported machine was 18.6quintal/hour this may happen duo to sieve difference.

3.2 Effect of Feed rate on Cleaning Efficiency and Cleaning loss

As we can see from test results, increasing the feed rate was caused decreased in cleaning efficiency. The declining cleaning efficiency and increasing cleaning loss with increasing rate of feeding was due to the formation of a thick layer of material on sieves that considerably hindered or limited passage of grains through the sieve perforations. The increasing in cleaning loss and decreasing of cleaning efficiency with increasing feed rate could be attributed the load intensity on the sieve that could result in matting of the sieve with material other

than grain blocking sieve holes. Furthermore, whenever there are high feed rate, the current supplied will not be capable of suspending and blowing the materials aerodynamically as multiple particles act as obstruction to airflow.

3.3 Participants views towards promoted technology

Participants were asked how they perceive to the new technology as compared to imported technology of seed cleaning machine in terms of its given features/ attributes like, easiness of utilization, appearance of the machine, import substitution, affordability of technology. Likert scale method was used to measure respondent's opinion/views towards the attributes of the new technology with respect to imported seed cleaning machine. A Likert scale is an ordered scale from which respondents choose one option that best aligns with their view. It is often used to measure respondents' attitudes by asking the extent to which they agree or disagree with a particular question or statement. In this case an odd number of response categories having five responses (strongly disagree, disagree, neither disagree nor agree, agree, and strongly agree) were used. All participants strongly agree with the easiness to utilize, import substitution, affordability of technology with respect to imported seed cleaning machine. Out of total of participants about ninety nine percent of participants strongly agree with necessity of import substitution.

4. References

Brandenburg, N. Robert, and Harmond, Jesse e. 1964. Fluidized conveying of seed. U.S.

Dept. of agr. Tech. Bui. 1315, 41 pp.

Brandenburg, N. R. 1961. A Velvet-Roll Separator for Seed Testing. U.S. Dept. Agr. ARS 42-53, 12 pp. July.

Brandenburg, N. R., and Booster, D. E. The Blakiston, Co., Inc., 626 pp. New York.

Ching, Te may., 1958. Safer seed storage. Crops and Soils 11(3): 16-17.

Cooper, H. W., Smith, James E., JR., and Atkins, M.D., 1957. Producing and harvesting grass seed. In the great plains. U.s. dept. Agr. Farmers' Bui. 2112, pp. 1-30.

Hall and Carl W., 1957. Drying farm crops. Agricultural Consulting Associates, Inc., 336 pp.

Harmond, Jesse E., 1966. Separating seeds by length with special Indent cylinders. Oreg. Agr. Expt. Sta. Tech. Bui. 88, 20 pp.

Henderson, S. M., and Perry, R. L. 1955. Agricultural Process Engineering.

K. J. Simonyan and Y. D. Yiljep, 2008. "Investigating Grain Separation and Cleaning Efficiency Distribution of a Conventional Stationary Rasp- bar Sorghum Thresher" Agricultural Engineering International: the CIGR Ejournal Manuscript PM 07 028. Vol. X.

Klein, L. M. 1961. Vibrator Seed Separator. U.S. Dept. Agr. ARS 42-50, 5 pp. February.

Computational Fluid Dynamic Simulation and Experimental Testing of a Serpentine Flat Plate Solar Water Heater

Gutu Birhanu O^a.; A. V. Ramayya^b & GetachewuShunki T^c.

^aOromia Agricultural Research Institute, Bako Agri. Engineering Research Center P.o.Box 07,Bako,West Shoa

^b Professor of Mechanical Engineering, Jimma University, Institute of Technology (JiT), P.O.Box 378, Jimma, Ethiopia

^c School of Mechanical Engineering, Jimma University, Institute of Technology (JiT), P.O. Box 378, Jimma, Ethiopia

Abstract

The aim of the study is to improve thermal performance of passive serpentine flat plate solar collectors using striped technique. Striped mechanism was applied on absorber plate so as to diminish thermal fusion in the plate and investigation enhancing practice of energy conversion from the collector units to the working fluid. Study was conducted or carried out with numerical simulation and experimental testing to compare results for validation. Demand of domestic hot water has mostly been filling with conventional flat plate solar collectors. Conventional solar collectors are relevant for high flow rate that requires high operational costs. In the past, serpentine solar collector was ignored due to large pumping requirements at higher flow rates. However at low flow rate, serpentine collector is more economical and efficient. Therefore, striped absorber plate of the serpentine solar collector in various modes were designed by ANSYS 14.5 release FLUENT and simulated using computational fluid dynamics. The effect of the configuration parameters of striped serpentine solar collector was investigated and good result was obtained. The analysis was done by decoupling the last striped from whole system. So that the result of the second stripe became inlet boundary condition for the last of four segments. For the collector mass flow rate of 0.00285kg/s and solar radiation of 650w/m², temperature of absorber plate (T_p) and water at collector exit (T_o) became 360k and 338k respectively. The same collector model was manufactured and experimental investigation was carried on with similar conditions as did for simulation. Therefore, absorber plate (T_p) and water at exit of the collector (T_o) during the experimental test attained maximum temperature of 353k and 336.9k respectively. Therefore, numerically predicted temperature distribution on the striped absorber plates was agreed with experimental obtained data with little discrepancy. This inconsistency was due to variance of solar radiation and data measurement error. Collector heat removal factors obtained with both numerical study and experimental testing was similar in figures and remarkable with other research.

Keywords: *Thermal breaking, serpentine flat plate solar collector, thermosyphone, CFD & Experiment*

1. Introduction

Solar collectors are special kind of devices that transform solar irradiance into internal energy of the transport medium, and hence increases their thermal effects. They absorb and capture the incoming solar radiation, converts it into heat and transfers the heat to a fluid flowing through the collector^[1]. Demand of domestic hot water has been satisfying with various heating application.

However, solar water heating alone reduced domestic water heating costs by as much as 70%^[2]. Flat-plate solar collector is the most common for residential water and space heating as well as for industrial application. Most of them currently available on the market are of the parallel tube type known as conventional flat plate solar collector^[3]. They are relevants for high flow rate that requires high operational costs. Moreover, conventional flat plate collector had been in service for a long time without any significant changes in their design, shape and operational principles^[4].

According to Matrawy & Farkas^[5] configuration of a solar collector is an important factor that determines its thermal performance. Serpentine solar collector has the potential to perform better than a conventional parallel tube collector in low-flow systems due to the earlier onset of turbulent flow which enhances heat transfer application. Even for the same collector area, tube spacing and tube diameter, serpentine collector performer better than conventional collector^[6]. According to Myrna & Beckman^[7] the major reason for the difference in performance between conventional and a serpentine flat plate solar collector was the internal heat transfer coefficient. However in the past, serpentine flat plate solar collector was ignored due to large pumping requirements at higher flow rates.

Serpentine collector has geometry for which collector efficiency factor and heat removal factor cannot easily be expressed in a simple form. If thermal break is made midway between the serpentine tubes, then the collector can be analyzed as a conventional collector. If the break is not provided, reduced performance can be expected and more complicated analysis is necessary^[8]. The heat removal factor for a serpentine collector is much more difficult to determine than for a conventional flat-plate collector^[7]. Unlike analysis for conventional collector, there is heat transfer between the tubes for a serpentine collector.

Several paper with analytical solutions were published. All analytical solutions were done to treat the differential equations governing the heat transfer in a serpentine-tube absorber. Abdel-Khalik^[9] found an analytical solution for heat removal factor of a serpentine tube bonded to the plate with two segments. He concluded that analytical solution for two segments was applicable for any number of segments with small error. Zhang and Lavan^[10] showed that this conclusion was lead to much errors than predicted for a certain parameter range by obtaining analytical solutions for $N=3$ and

4. The solution ignores heat transfer application through its U-bend portion and assumes one-dimensional heat transfer in the plate.

Chiou & Perera^[11] also analyzed the serpentine collector for any number of turns. As the number of turns increases, value of heat removal factor (FR) approach the values for turn $N=1$. In this case, the analysis for a long straight collector with no turns will hold. Therefore, the model is very close to the model for the flat plate collector, with the exception being that the internal heat transfer coefficient will be different ^[6].

There are only a few publications that report on experimental results of serpentine-flow solar collector. Eisenmann & Wiese^[12] had conducted experiment on two serpentine collectors that have the same geometry and shape. In the first collector, serpentine tube was soldered to the absorber plate all through the collector, whereas in the second collector bends of the tubing was not thermally connected with the absorber. They put both over the sun under identical meteorological conditions and measured their performance. The efficiency of the collector that was soldered to absorber plate became about 2 to 2.5% superior in the experiment.

The experiment was conducted on the collector whose absorber plate was soldered to serpentine tube rather than striped plate that attached to tube. In fine and tube absorber collector arrangement, heat is normally transferred through absorber plate to tubes and then working fluids. As result, thermal diffusion due conduction mode caused throughout the system which reduces overall performance in the collector. Moreover, the experiment was unable to make predictions on the required parameters UL & F' of a serpentine-flow collector experimentally. Unlike parallel flat plate collector, there is heat transfer occur between tubes for a serpentine collector resulting in two dimensional heat transfer problem. Thus, it requires thermal break midway between serpentine tubes, and then the collector can be analyzed as a conventional collector. Consequently, coarser approximations need to be made in order to achieve analytical solutions for the absorber and fluid temperatures (Lund, 1989)^[13] as cited by Eisenmann & Wiese.

Since computational fluid dynamics analysis of the flow and heat transfer in flat plate solar collectors is computationally quite difficult and cost, number of research works on this subject is quite low^[2,14]. However, there was no adequate simulation work has been done so far for a serpentine collector. Thus, it was designed to perform simulation and experimental testing of serpentine flat plate solar collector. It is obvious that there might be certain limitations for experimental results thus data at each and every point but computational fluid dynamics (CFD) handles complex situations where experimental is not applicable because of limitations and cost effectiveness problem^[15].

2. Material and Methodology

Geometry model was designed using ANSYS and the model get transferred to mesh. In meshing section, parameters of geometry part was defined. For better thermal and flow analysis, under mesh sizing, fining was selected to discretize flow further in to many

elements and updated to recognize the input. Similar model was designed, manufactured and assembled for the experimental test. Thermocouple sensors were provide on serpentine tube and the plate in order to gauge thermal and flow distribution through the collector. Collector site orientation was adjusted and temperature distribution through the plate as well as water in the tube recited with digital multi-meter reader.

2.1 Development of Geometry & Meshing

Basic serpentine flat plate solar water heater was developed and going to be investigated. Unlike conventional collector, there is a complicated heat transfer network present in between serpentine tubes in the collector which results the analysis into 2-D heat transfer problem. Therefore, it is not easy to do the analysis of flow and thermal character inside the tubes and absorber plate. Thus, it requires appropriate thermal breaking application in the system. Breaking in the midway was one of the option but using more breaking system cause further complication on the setup of the boundary condition for decoupling and/or coupling system.

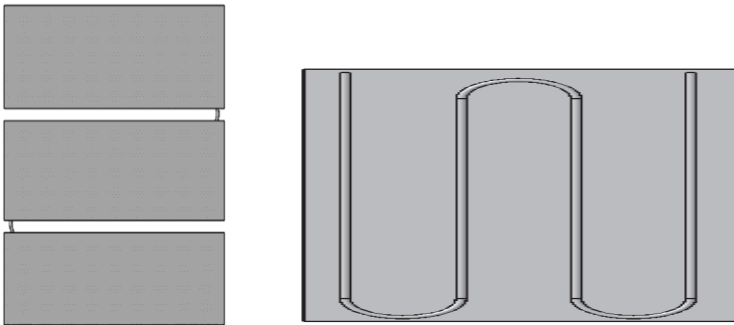


Figure 1. How designed striped geometry was decoupled from main system

Geometry employed for numerical investigation was illustrated as above and two thermal breaking lines were applied to simplify the analysis. The breaking lines are 20mm apart which separate adjacent plates adequately for possible losses occur due to heat conduction and moreover 20mm thick Styrofoam insulation was used in between two consecutive striped plates. Development of an exact computational mesh for the domain under investigation was paramount importance in CFD simulations. The accuracy of numerical results in CFD modelling was mesh dependent that means the finer mesh generally provides better results at the increased computational time [16]. Therefore the size of the mesh in the domain should be gradually increased to such level that the further raise in the number of control volumes does not result in considerable changes in theoretical or imaginary results obtained at the end of the exploration.

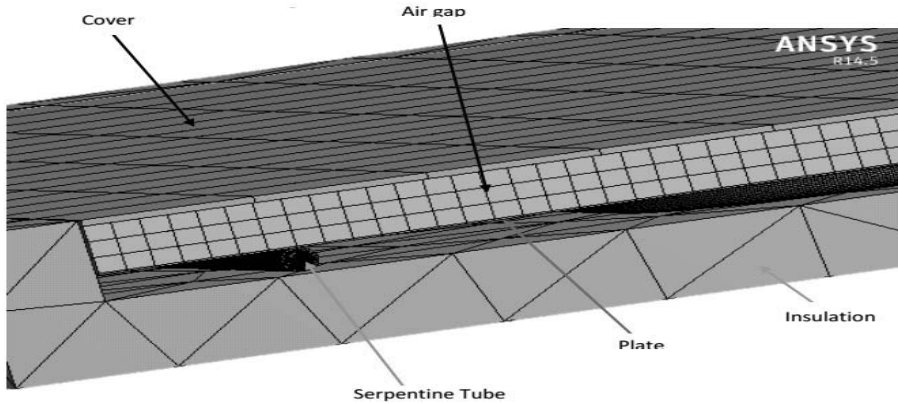


Figure 2. Computational grid of the system

Properties of materials employed for model were activated from the domain. The properties of water was used for a liquid domain in the computational mesh. Piecewise-linear functions were used to make into account the dependence of water properties upon temperature. The effect of gravity was taken into account along the vertical axis by specifying the negative acceleration value. Since flow was very small, laminar flow model with pressure-velocity coupling used.

The radiation heat loss to the sky was included in the boundary condition of the side wall and glass cover. The apparent sky temperature was calculated by using the equation from ASHRE hand book^[15]. Heating of surfaces due to radiation and/or heat sources within the fluid phase can be included in this model. There are five radiation models which allow us to include radiation, with or without a participating medium in heat transfer simulations.

Solar load model are used to calculate radiation effects from the sun’s rays that enter a computational domain. The model includes a solar calculator utility that can be used to construct the sun’s location in the sky for a given time-of-day, date, and position. Solar load is available in the 3D solver only, and can be used to model steady and unsteady flows.

2.2 Prototype Manufacturing

Similar model of serpentine solar collector was manufactured with striped techniques where the plate was attached to serpentine shaped tube for separated segments. Striped mechanism prohibited or minimize intensity of thermal losses through the collector active part without doing the required work. Thermocouple sensor was provide on serpentine tube and the plate in order to gauge thermal and flow distribution through the collector.

Heat losses to neighbor or adjacent side of the collector system with conduction and convection processes. To interact with losses, thermal breaking line was formed between

two adjacent plates with about 20mm part. That thermal line was covered with Styro-foam material which serve as insulator for heat to minimize air circulation in the collector. Since the collector rely on natural circulation system, significant amount of heat can be gained due to unique property of low flow rate.



Figure 3. Physical feature, how serpentine tube bend to required shape & kept in collector system

2.3 Experimental setup

Experiment setup was established in Jimma Agricultural Mechanization Research Center Lab and testing was conducted for over one month with outdoor condition. The collector was designed with two thermal breaking lines that divided the collector into three striped real model. And all the collector units were kept over the sun to trap incident radiation. Serpentine tube was soldered to the absorber plate to enhance thermal flow in favor of contact with aluminum sheet that has 0.8mm thickness. They are used to establish good heat transfer application between absorber plate and the tube and also insist heat transfer process from plate to transport fluid.

2.4 Collector Orientation

The collector position was adjusted to best performing angle of orientation. This should be as close as possible to Due South (0°) in the Northern Hemisphere for absorption of maximum solar irradiation. The surface orientation leading to maximum output of a solar energy system may be quite different from the orientation leading to maximum incident energy. The total annual energy received as a function of slope is maximum at approximately $\beta = \phi$ where ϕ is the latitude. For maximum annual energy availability, a collector tilt angle equal to the latitude is considered ^[8].

The performance of the solar water heater depends on prompt exposure to incoming solar radiation. Therefore, the solar collector should be far from block obstacles like tall buildings, trees or hills positioned in front and back side that hindered them to gain substantial solar energy.

Table 1. Collector Specification

No	Parameter	Symbol	Magnitude
1	Length of one serpentine segment	L	0.96m
2	Distance b/n tubes	W	0.14m
3	Plate thickness		0.8mm
4	Tube outside diameter	D	12.7mm
5	Tube inside diameter	Di	11.28mm
6	Plate thermal conductivity	k	46 w/m0c
7	Mass flow rate of water		0.0028kg/s
8	Collector area	Ac	1.52m ²
9	Collector slope angle		100
10	Space b/n plate & glass	-	20mm
11	Thickness of back insulation	L _b	0.046m
12	Back insulation thermal conductivity	Kb	0.02w/m 0c
13	Thickness of collector	-	0.085m

3. Result and Discussion

3.1 Introduction

Under computational fluid dynamics case, solution was found and the required parameters were displayed in post-processing. Here by using CFD software temperature distribution inside flow tube and absorber plate of serpentine collector were predicted thereby to estimate collector efficiency factor and other parameters that express collector performance. Here flow characteristics and thermal performance of the serpentine solar collector was examined by experimental testing. Temperature distribution through the plate and working fluid has been followed with K-type thermocouple sensors. The sensor displayed the input in the form of voltage and the voltage was translated in to temperature using standard table.

Eventually, the result obtained with computational fluid dynamics simulation analysis was compared with experimental testing outcome for validation purpose.

3.2 CFD simulation

The numerical results obtained from CFD modelling of a serpentine solar collector model is presented as follow. As it was tried to explain in earlier, the collector system was divided in to three stripes because of thermal breaking system. Each striped model was engaged with detail operational and boundary condition considered for best simulation purpose. The properties of copper, aluminum and glass were applied for tubes, absorber plate and cover system respectively.

The properties of water were temperature-dependent and piecewise-linear functions were used to take into account dependence of water properties upon its temperature.

On top surface of absorber plate, equivalent heat fluxes of 650W/m^2 was applied. Providing that the side and the bottom part of the plate was set to be at adiabatic condition. This heat flux was calculated from average based of solar radiation collected on June 30, 2014. For both CFD and experimental testing, heat fluxes of 650W/m^2 was used to simulate temperature distribution though out absorber plate and water flow through the tube.

Collector thermal analysis was generally performed in the following ways. The first striped model was simulated with a given boundary conditions and output condition of this model coupled and decoupled to become input for the next stripe. Again the output of the second striped model was coupled and again decoupled to the last striped. In such away the solution for serpentine flat plate collector was analyzed until the result obtained become dissimilar. Figure5a demonstrated the temperature distribution pattern of the water in the tube for the last decoupled striped model.

This methods may works or be easy for fluid flow in the collector tube but might be difficult or may has limitation concerning with air, cover and insulation material that were thermally broken for analysis. For this case, uniform boundary conditions for air, cover and insulation were used for all stripes. For instant, wall boundary conditions with convection heat transfer coefficient of $20\text{ w/m}^2\text{k}$ was applied for air in all stripes. Because of the serpentine solar collectors was set to be inclined to horizontal, the effect of gravity was taken into account along the vertical axis by specifying the negative acceleration value of cosine 10° multiplied by the gravitational forces constant^[16]. Collector angle was established based on recommendation made with literature. Experimental site has latitude of 7.7° and collector angle was made to be 100 for best annual solar radiation collection option without applying tracking system.

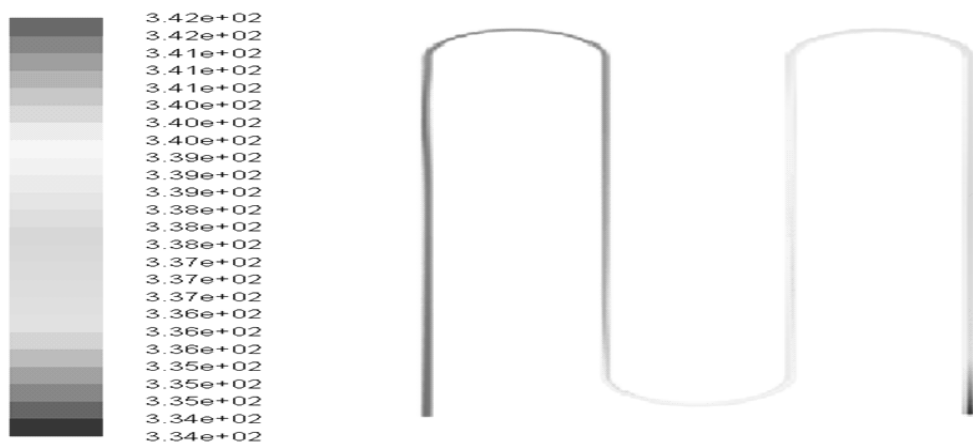


Figure 4. Temperature contour of the last striped serpentine tube

Figure 4 presents the temperature contours of water in the tube. As it can be seen from the graph, the water entered the serpentine tube of the last striped at an inlet temperature of 334k (which is exit temperature of second striped). Gradually as the flow passes through the tube, the temperature of the fluid at the exit of the tube became 342k. This result showed that there was better heat transfer process in the system. The numerical results obtained clearly demonstrate that the proposed design of the solar collector provides a considerable improvement of the performance.

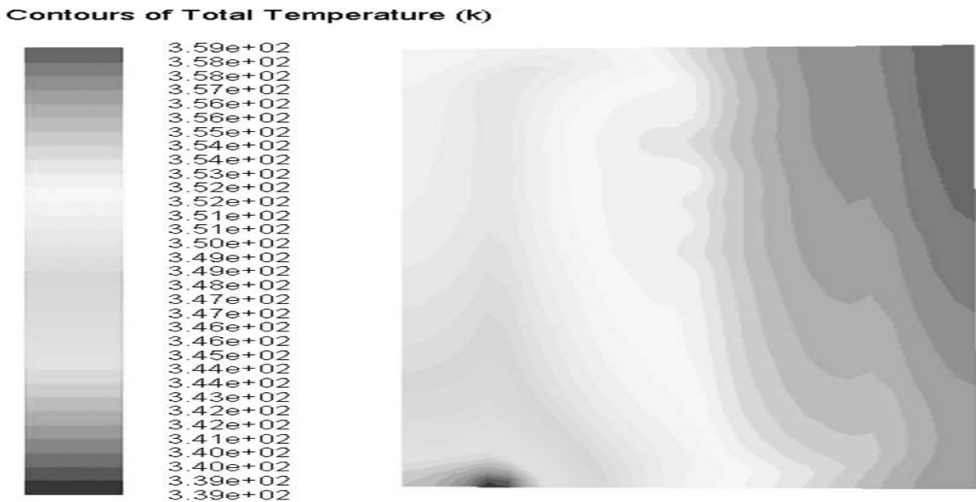


Figure 5. Temperature contour of the last striped absorber plate

Absorber plate has achieved maximum temperature of 360k that was small as compared with some literature. This was because solar radiation available during the time of experimental testing was of the smallest of the all months. In general, the test was conducted during the summer season when availability of constant solar radiation was inconvenient. Meanwhile as you increase the heat flux more and more, thermal distribution through the system became higher.

The same amount of solar heat flux was used to examine collector performance thoroughly for both numerical and experimental test activities. Since the main aim of this research is to investigate thermal performance characteristic of the serpentine flat plate solar collector with CFD simulation and experimental testing, similar condition has to be applied to perform comparison.

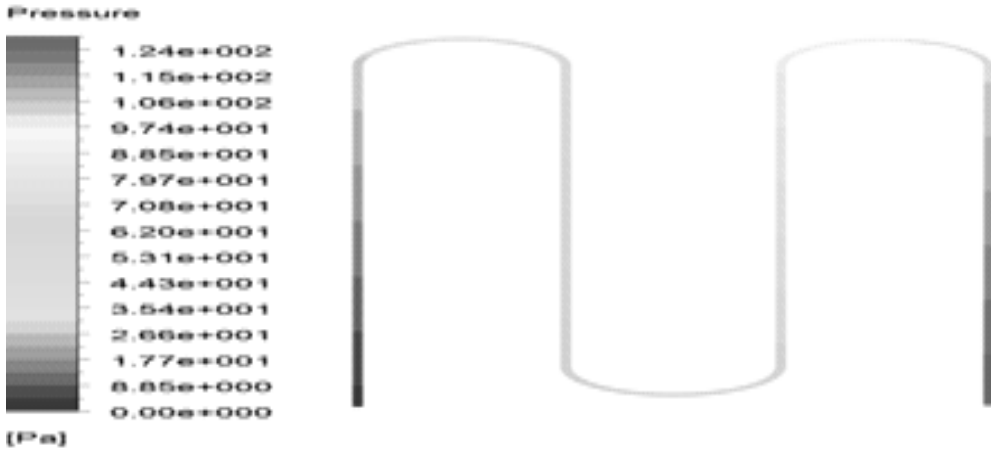


Figure 6. Pressure drop of water flow in serpentine tube of the last striped

As it can be seen from the Figure 6, high pressure drop was seen at collector inlet. Water moves down from the storage tank to the collector due to gravity but as soon as it leaves tanker and reach the inlet section, it faces the bend that become obstacle to flow.

As result it losses energy which causes pressure drop at the section. In general, pressure drop seen was an order of 124 Pascal. Only the last decoupled four segmented striped was analyzed here, in fact pressure drop through serpentine tube is higher when compared to conventional one.

The flow in the collector was induced by the density gradient, which in turn was caused by the heating of the working fluid. The figure in general shows the typical variation of the density inside the collector.

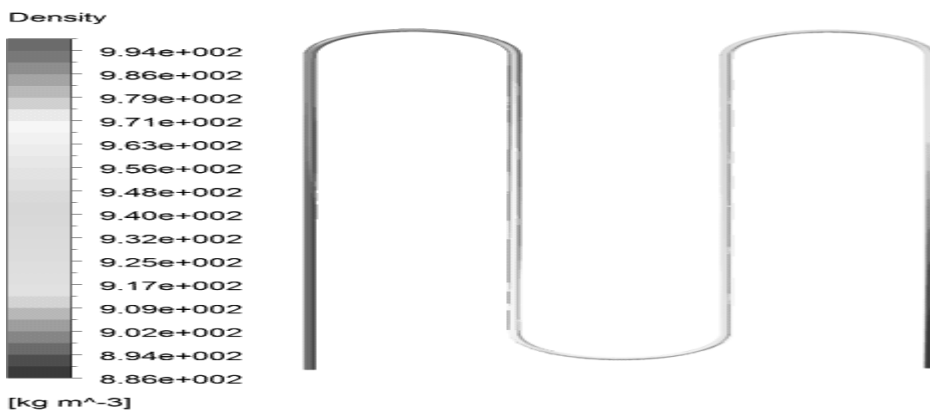


Figure 7. Density contours of water in serpentine tube

It can be seen that for the given boundary conditions the density of water changes from 886 kg/m³ at the top after heating process to 994 kg/ m³ at the bottom where the temperature is the lowest. Also from numerical results the water is cold more at the collector inlet section since higher water density results represent a lower water temperature in collector tube.

3.3 Leak test result

On the serpentine tube hole was prepared and the thermocouple sensor was attached with help of epoxy materials. Unless the sensors were attached with drilled holes tightly to tube, leak probably occur. Therefore to minimize the tendency of the leak, leak test was conducted with water-immersion methods. Leak was general omitted from water flow through the tube in whole collector system.

The smallest bubble an operator could detect has 1 mm radius and that the waiting time is 30 seconds^[17]. Assuming that the pressure inside the bubble is at atmospheric pressure, it can be stated from the previous equations that the bubble volume is and therefore the minimum detectable leak rate at Jimma atmospheric condition become

3.4 Estimation of Solar Irradiance

The thermal performance of natural circulation solar water heating was tested on June 30, 2014 at Jimma Agricultural Mechanization Research Center using serpentine flat plate solar collector setup with batch type water tank. An estimation of solar isolation of that experimental site was made by employing engineering equation solver (EES) software. A program that compromised important parameters of air with non-dimensional units was developed. Data’s were collected on the temperature of air, sky and black body with ten minute intervals. Since once the program was developed, the collected data was inserted in the program and manipulated. Figure 8 shows the profile of solar radiation available that was calculated based on data of the test day. Since season was summer, it has been difficult to get a clear day to do performance test and several trials have been done to get good daily solar curve. This data was one of the best clear days for performance test.

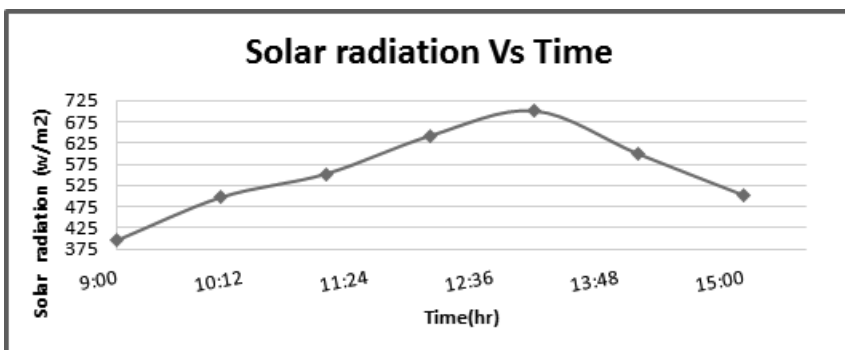


Figure 8. Solar radiation on June 30, 2014 at Jimma Agricultural Mechanization Research Center

Due to decreases in solar radiation, the ambient temperature also starts to decrease. Ambient temperature variation of the experimental site also has the following pattern.

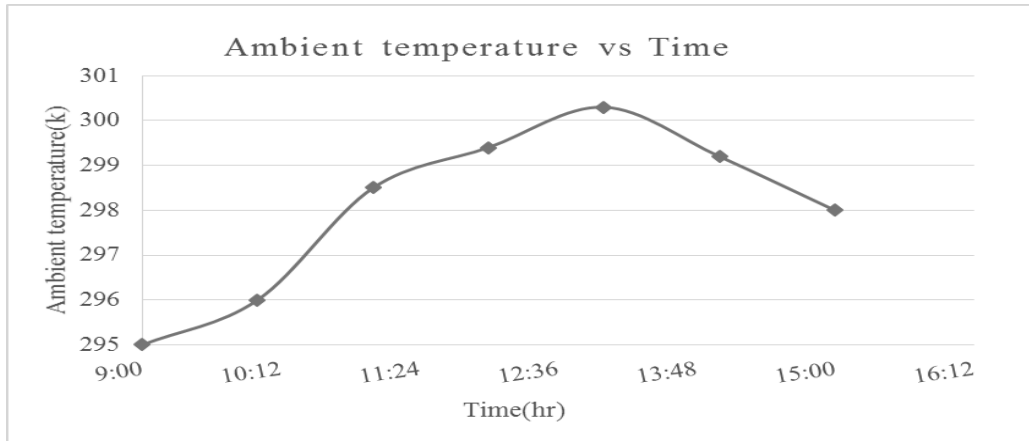


Figure 9. Ambient temperature variation of the experimental site

3.5 Experiment result

Temperature distribution through the plate and water in the tube were measured using k-type thermocouple. Since the thermal breaking system was applied, absorber plate was detached from each other and fixed to tube with soldering techniques. On the serpentine tube, this temperature sensors were attached on holes so as to read temperature distribution through the flow. In addition, the sensor was attached on the surface of plate to measure how hot could absorber surface be.

Table 2 below displays temperature of water flow in the serpentine tube. The collector system was divided into three stripes as result of thermal breaking application and on each strip as per the thermocouple sensor allocated, data has been registered with in 20 minute intervals. Different reading of temperature was recorded at every hour and average values of water temperature are considered. Here temperature was read in terms of voltage induced caused due to temperature difference between conducting wires in sensor. Using this induced voltage, corresponding temperature was read using standard table including ambient temperature.

Table 2. Temperature of water in the tube at various points

Z(m)	0.09	0.16	0.30	0.42	0.56	0.83	0.97	1.12	1.26	1.48
	1.47	1.52								
X(m)	-	0.48	0.93	0.03	0.93	0.48	0.03	0.48	0.93	0.48
	0.03	0.93								
T _w (K)	295	298.2	302.5	317.4	317.6	319.3	320.7	322.9	323.3	323.5
	336.9	317.4								

Table 3 displayed average plate temperature distribution in the absorber plate. Temperature of the plate was computed on average based and displayed here at every ends of the strips. Four temperature values were shown as per the stripes.

Table 3. Absorber plate temperature at various points

Z-axis(m)	0.295	0.68	1.15	1.55
X-axis (m)	0.45	0.57	0.35	0.48
Plate temp(k)	334	345	351.5	348

Heat removal factor of the collector (FR) can also be calculated for the experimental testing. Collector inlet temperature of the water was estimated from experimental testing and become 293k and collector exit temperature is 336.9k as well as mean temperature plate is 351.5k from collector experimental data. Therefore, UL becomes 4.98w/km² and F_R becomes 0.780878.

Table 4. Collector removal factor at solar heat flux of 650w/m²

Parameters	CFD	Experimenta	Analytical
Heat removal (F _R)	0.8783	0.7809	0.8190 (Al)
Efficiency factor (F')	0.7476	0.5879	-

Figure 10 indicated that how temperature of the flow was varied with location. This figure displays temperature distribution of water flow in tube along z-axis. Water was admitted to the inlet of collector at temperature value of 20 °C. As it passes through the tube, heat transfer takes place so that water start gaining considerable heat from the process. As it can be seen from the graph, the water in the tube extract little amount of heat in first strip since it goes short distance to complete loop.

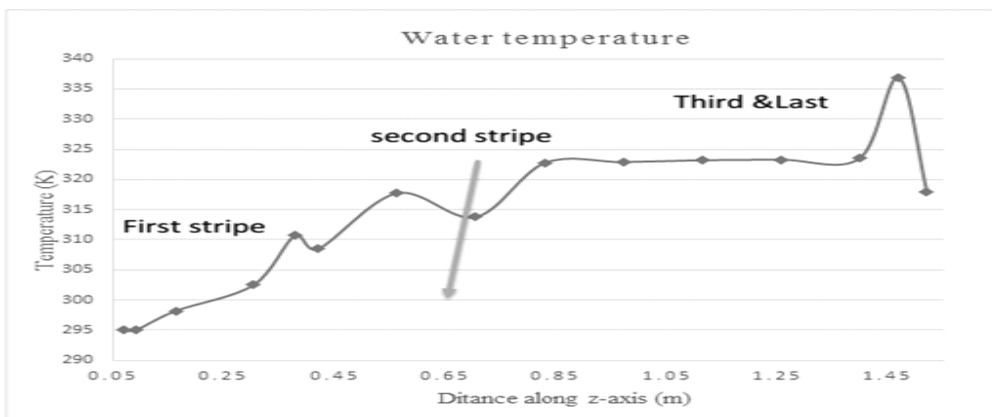


Figure 10. Temperature variation of water in the collector

In the above diagram, the maximum temperature of the water in the first strip was 310k but as it passed to the next strip, considerable amount of heat was enabled to be gained. Due to possibility of long contact time with the tube surface that causes good heat transfer process in the system. As result, water in the tube gained significant amount of heat. The water in the tube attained maximum temperature of 337k throughout the system. Figure11 displayed below demonstrated collector plate temperature distribution in whole strips. Temperature variation is taken in average based at each end of the strips. In second and third strips, collector plate temperature was sharply increasing and attain maximum temperature of 351k at the middle third strips. Here solar radiation directly fallen on the absorber plate and there was no apparent shading effect. For last strips, there is possibility of self-shading effect for time before noon. Even though water storage tank was suited above the collector, it affected thermal performance of the last strip. The graph is drawn using result obtained at 14hr.

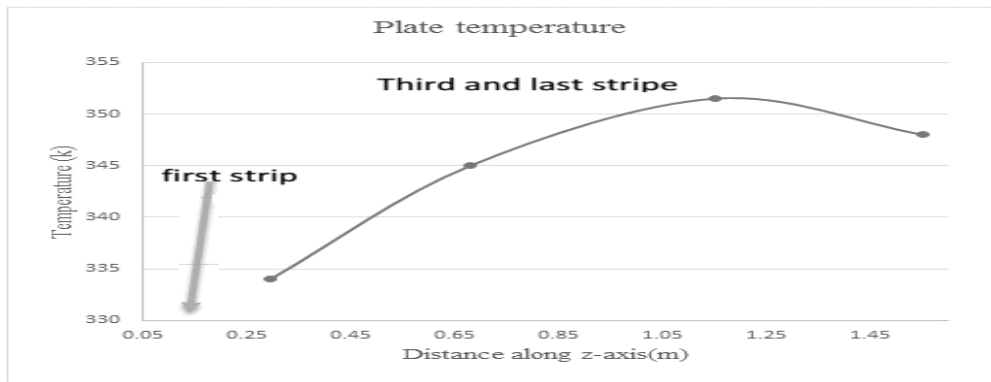


Figure 11. Temperature distribution in absorber plate

Table 5 below has displayed the summary of water of temperature at tube exit obtained by CFD simulation and experimental testing .The data’s were kept here to comparison the result obtained with both simulation and testing.

Table5. Summary of comparison of water temperature in tube obtained by Computational Fluid Dynamics & experimental result

Time (hr)	Solar Intensity (w/m2)	Amb Temp(k)	Water temp by CFD(K)	Water temp by experiment(k)
9:00	396	295	315	305
10:00	497.6	296	320	317.73
11:00	552.2	298.5	322	313.73
12:00	641.8	299.4	326	322.77
13:00	648.6	300.3	328	323.38
14:00	700.5	299.2	338	336.9
15:00	562.5	298	320	318.43

Figure 12. Comparison of temperature of water at collector exit with CFD & experimental

Collector instantaneous efficiency was found to vary according to the external conditions i.e. solar radiation, ambient temperature and mean tanker temperature. The efficiency curve of experimental results agreed with model. The collector system showed higher efficiency at low tank temperature and the efficiency decreases as the tank temperature increases. An average tank temperature was 322k and $FR\tau\alpha$ is the y-intercept in the efficiency line and FRU_L represents the slope of the curve. The higher the slope, the higher is the sensitivity to external conditions. Both experimental and model collector curves have high slope value which indicates the efficiency is very sensitive to external condition. The heat transfer coefficient U_L also depends on the mean plate temperature.

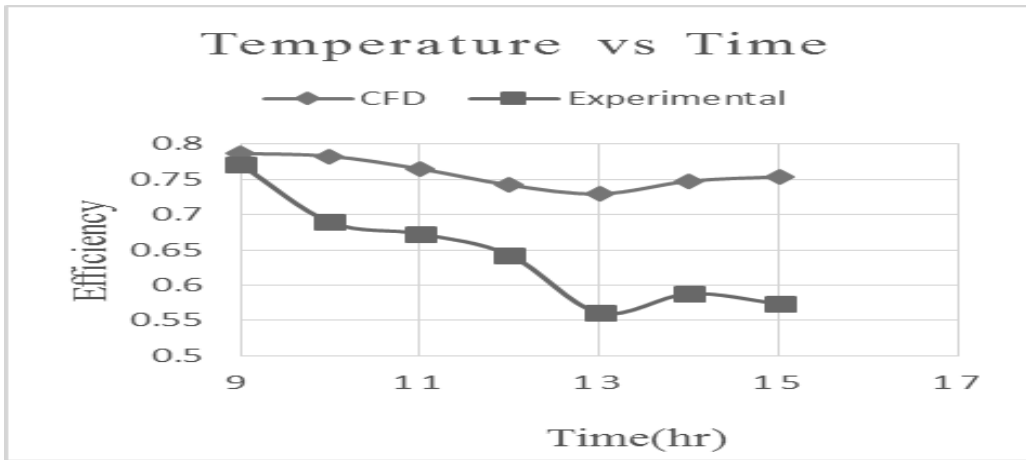


Figure 13. Collector Instantaneous efficiency during test hours

Khalifa^[18] experimentally investigated the impact of mean plate temperature on the total and collector top heat transfer coefficient. It was found the total and collector top heat transfer coefficient varies during the test hours due to the increase solar radiation and the mean absorber temperature. Higher collector inlet temperature increases the mean plate temperature and increases the collector total heat transfer coefficient which reduces the efficiency of the collector.

4. Conclusion

Thermal performance of flat plate solar collector can be improved by altering its configuration of heat transport system from solar absorber to heat storage system. Solar collector size, shape and flow rate in general affect system performance. Serpentine flat plate collector was designed based on thermal breaking system that was recommended by different literatures. Unless thermal breaking was applied, it is difficult to model formulae that enable to analysis as conventional collector. The performance of this collector was investigated by numerical simulation methods. Collector model was designed applying ANSYS 14.5-FLUENT software. The software was used to identify the optimum configuration of the most economical serpentine flat plate solar water heating systems.

For the collector mass flow rate of 0.00285kg/s and solar radiation of 650w/m², temperature of absorber plate(T_p) and water at collector exit (T_0) became 360k and 338k respectively. The same collector model was manufactured and experimental investigation was carried on with similar conditions as did for simulation. Consequently, absorber plate (T_p') and water at exit of the collector (T_0') during the experimental test attained maximum temperature of 353k and 336.9k respectively.

Collector model has three stripes and while both CFD simulation and experimental test was taking over, all stripes exhibited varies temperature distribution in the collector system. For experimental session, solar radiation is directly fallen on the absorber plate and there is no apparent shading effect seen especially for the time before noon in second stripes whereas in third and last stripes, there is possibility of self-shading effect observed for time before noon. Even though water storage tank was suited above the collector, it affected thermal performance of the last strip. Consequently, such temperature variation was happened in the strip.

In general, numerical and experimental results obtained were found with good agreement with some deviation. In numerical case, serpentine flat plate solar collectors outperformed better when compared to experimental due to some experimental imperfectness during data collection and instant variation of solar insolation. Numerical results obtained demonstrated that striped absorber plate design would improve the heat transfer from the walls of tubes to the liquid which results hot water production of the solar collector good.

5. Recommendation

Serpentine solar collector requires further study to model the science exist behind the collector. So far different studies were conducted on the collector to model collector's important parameters using analytical methods for several turns. Yet modeled collector heat removal factor (FR) formula was invalid for all materials.

As we all know that serpentine solar collector has geometry for which collector efficiency factor and heat removal factor cannot easily be expressed in a simple form. Unlike the analysis for the parallel flat-plate where the fins between the tubes are assumed adiabatic at the center of the tube spacing, there is heat transfer occur between the tubes. However no analytical modeling was formulated for collector efficiency factor for serpentine solar collector. It is unable to make predictions on the thermal output of a serpentine-flow collector with experimental.

Thermally breaking the collector system in to more than two stripes requires serious attention in settling required boundary conditions. In this research, two thermal breaking line was applied and each stripe was analyzed separately and later coupled. Accordingly, output of the first stripe became input for the second stripe and output of the second stripe became input for the third stripe. In such manner, analysis of collector system was done and finally coupled together to become the collector system. This methods may

works for fluid flow in the tube but might be difficult with air, cover and insulation material that were thermally broken for analysis. Therefore, more effort is required to model (F') to analyze the thermal behavior of the tube bends. Moreover, detailed numerical investigations should also be taken into consideration.

Bibliography

- [1]. Soteris A. Kalogeria, 2009. Solar Energy Engineering Processes and Systems Book, first edition, TJ810.K258, USA
- [2]. Mohamed Selmi, Mohammed J. Al-Khawaja, Abdulhamid Marafia, 2008. Validation of CFD simulation for flat plate solar energy collector, Renewable Energy 33 (2008) 383–387.
- [3]. N. Molero Villar, J.M. Cejudo Lo'pe, F. Domínguez Muñoz, E. Rodríguez Garcí'a, A.Carrillo Andre's;2009. Numerical 3-D heat flux simulations on flat plate solar collectors, Solar Energy 83 (2009) 1086–1092.
- [4]. P. Sivakumar, W. Christraj, M. Sridharan and N. Jayamalathi,2012.Performance improvement study of solar water heating system, ARPN Journal of Engineering and Applied Sciences,Vol.7,No 1,pp 45-9.
- [5]. Matrawy, K.K., Farkas, I., 1997. Comparison study for three types of solar collector for water heating. Energy Conversion and Management 38, 861–869.
- [6]. Dayan Myrna, 1997. High performance in low-flow solar domestic hot water systems thesis.
- [7]. Myrna D., Sanford K. & William Beckman, 1998. Analysis of serpentine collectors in low flow systems, Solar Energy Laboratory University of Wisconsin-Madison 1500 Engineering Drive Madison, WI 53706
- [8]. John A. Duffie & William A. Beckman, 1991. Solar Engineering of Thermal Processes, Second edition, Wiley-Inter science Publication John Wiley & Sons, New York.
- [9]. Abdel-Khalik S.I., 1976. Heat removal factor for a flat-plate solar collector with a serpentine tube, Journal of Solar Energy Vol 18, pp59-64.
- [10]. Zhang H.-F. & Lavan Z., 1985. Thermal performance of a serpentine absorber plate, Journal of Solar Energy, Vol. 34, pp175-177.
- [11]. Chiou, J.P. & Perera, D.G.; 1986.Non - Iterative Solution of Heat Transfer Equation of Fluid Flowing through a Serpentine Tube attached to a plate with radiation as a heat source, American Society of Mechanical Engineers-Heat Transfer Division, Vol62, pp. 89- 96, ASME, New York.

- [12]. Wolfgang Eisenmann, Frank Wiese, Klaus Vajen & Hans Ackermann, 2000. Experimental investigations of serpentine-flow flat-plate collectors, Philipps-Universität Marburg, D-35032 Marburg, Germany.
- [13]. Lund K. O., 1989. General thermal analysis of serpentine-flow flat-plate solar collector absorbers, Solar Energy Vol. 42, pp133-142
- [14]. P.W. Ingle, A.A Pawaer, B. D. Deshmukh and K.C. Bhosale, 2013. CFD analysis of solar flat plate collector, International Journal of Emerging Technology Advanced Engineering, Volume 3, Issue 4, pp 337-42.
- [15]. ASHRAE Hand Book, 2011.HVAC applications, SI edition Supported by American Society of Heating, Refrigerating and Air-conditioning Engineers Research.
- [16]. IORDANOU GRIGORIS, 2009. Flat-Plate Solar Collectors for Water Heating with Improved Heat Transfer for Application in climatic Conditions of the Mediterranean region.
- [17]. VTech Leak Detection Methods, 2005. A Comparative Study of Technologies and Techniques Short version, USA.
- [18]. Khalifa, A-J. N., 1999. Thermal performance of locally made flat plate solar collectors used as part of a domestic hot water system. Energy Conversion & Management, 40:1825-1833.